Antibiotic-Induced Anomalous Statistics of Collective Bacterial Swarming

Sivan Benisty, Eshel Ben-Jacob, Gil Ariel, and Avraham Be'er

Phys. Rev. Lett. **114**, 018105 — Published 6 January 2015

DOI: 10.1103/PhysRevLett.114.018105

Antibiotic-induced anomalous statistics of collective bacterial swarming

Sivan Benisty,[1] Eshel Ben-Jacob,[2,3] Gil Ariel,[4] and Avraham Be'er[1]

[1] *Zuckerberg Institute for Water Research, The Jacob Blaustein Institutes for Desert Research, Ben-Gurion University of the Negev, Sede Boqer Campus 84990, Midreshet Ben-Gurion, Israel*
[2] *School of Physics and Astronomy, Raymond and Beverly Sackler Faculty of Exact Sciences, Tel Aviv University, Tel Aviv 69978, Israel*
[3] *Center for Theoretical Biological Physics, Rice University, Houston TX 77025*
[4] *Department of Mathematics, Bar-Ilan University, Ramat Gan 52000, Israel*

(Dated: December 16, 2014)

Under sub-lethal antibiotics concentrations, the statistics of collectively swarming *Bacillus subtilis* transitions from normal to anomalous, with a heavy-tailed speed distribution and a two-step temporal correlation of velocities. The transition is due to changes in the properties of the bacterial motion and the formation of a motility-defective sub-population that self-segregates into regions. As a result, both the colonial expansion and the growth rate are not affected by antibiotics. This phenomenon suggests a new strategy bacteria employ to fight antibiotic stress.

PACS numbers:

Bacterial swarming is an efficient mode of surface translocation, in which densely-packed, rod-shaped flagellated bacteria migrate within a thin layer [1–7]. Collectively moving bacteria often exhibit a coordinated dynamical structure of coherent whirls and flows, stemming from long-range hydrodynamic interactions and short-range steric forces [8–28]. Swarms may serve as a model for an active living matter with properties of a non-Newtonian nematic liquid [8]. In particular, they are essentially different from inanimate systems. Recent theory on self-propelled rods have demonstrated a reduction of the medium viscosity [9], dissipation of energy at the cell-scale [10], and a decrease of correlation time of the velocity field with increasing swimming activity [11]. Experimentally, the velocity and vorticity fields can be extracted using optical flow (OF) or particle image velocimetry (PIV) analyses. Previous studies agree that in rich conditions the dynamics is Boltzmann-like, i.e., the distribution of velocities is Gaussian, with an exponential decay of spatial and temporal correlations, indicating a Markovian process [11–13].

Bacteria developed collective survival strategies to cope with the adverse conditions of the wild. This motivated research efforts to explore the dynamical properties of collective behavior under a variety of adverse conditions, such as decrease of oxygen [14], nutrients [15] and water availability [3, 16]. It was found that while the mean bacterial speed typically decreases in response to stress, the swarming statistics remains qualitatively similar. In particular, the statistics of individual velocities remains Boltzmannian [11–13] and correlation times scale linearly with the swimming speed [14]. Here we report that antibiotic stress does lead to qualitative changes in the swarming statistics.

Recently, it has been demonstrated that swarming bacteria exhibit an elevated resistance to antibiotics [17, 18]. This was linked specifically to swarming motility and not to other types of movement. In particular, it cannot be attributed to antibiotic-resistant mutants [19]. The link between swarming and antibiotic resistance raises the inverse question: how does antibiotics affect the physical properties of the swarming dynamics. Understanding these effects may shed light on the mechanisms underlying these two processes.

In this work we show that the effect of antibiotics on swarm dynamics is fundamentally different than any of the other stress-inducing situations previously studied. When exposed to sub-lethal concentrations of kanamycin, the collective dynamics of *Bacillus subtilis* transitions from normal to anomalous behavior, with a heavy-tailed velocity distribution and a two-step temporal relaxation decay of the normalized velocity field. We find that this anomalous, non-Boltzmann dynamics is caused by the formation of motility-defective sub-population that self-segregates into clusters. This observation is verified both experimentally, using a mixture of motile and immotile *B. subtilis* cells, and theoretically, using simulations of a mixture of driven inelastic spheres.

The experimental setup. Experiments were performed on *B. subtilis* strain 3610, a wild type (WT) model species for swarm studies. Cells are rod-shaped (0.8×5 μm) with a rotating flagellar bundle at one of their poles that generates the thrust for the motion on the agar.

Agar-plates (1 g/l peptone) were inoculated with overnight culture (5 μl drops) resulting in multilayered, crowded, circular colonies. Optical microscopy (Zeiss Axio Imager Z2; 60X lens) and a high resolution video camera (GX 1050, Allied Vision Technologies; 100 fps and 1024×1024 pixels) were used to track the microscopic motion. See Supplemental Material (SM). Figure 1a shows a snapshot of swarming bacteria at the edge of a colony where the bacterial activity is maximal. Figure 1b shows the instantaneous velocity field of the same frame obtained by an off-the-shelf OF algorithm. Bac-

teria grown on antibiotics-free plates exhibited collective motion in the form of whirls and flows, as seen in similar bacterial systems, with a Boltzmann velocity statistics.

Kanamycin is a translation inhibitor antibiotics. In other words, it inhibits cell activities by stopping or slowing down protein synthesis. For example, it may reduce production of flagellin and disrupt the building of flagella (the motive organelle that enables swarming) and hence impair cell motility. Most biological antibiotic-related studies use lethal doses, in which the killing or inhibition mechanisms are relatively well understood, mostly at the single cell level. In contrast, in this paper we analyze the physical response of the swarm as a group, rather than observing the phenomenon at the single cell level. In our experiments, introducing kanamycin at low, sub-lethal concentrations ($0 - 0.1$ μg/ml) significantly changes the swarming dynamics. Comparing the velocity field of bacteria with and without added antibiotics, as depicted in Figure 1, it is evident that kanamycin reduces motility. However, sub-lethal concentrations do not affect the overall growth rate of the colony. In particular, we did not detect any added cell death. Figure 2a shows the number of colony-forming-units (CFU) at the swarm edge and the radius of the colony as a function of antibiotic concentration. Both are not affected by the added antibiotics at concentrations lower than 0.08 μg/ml.

Quantitative analysis of experiments. The mean speed of the cells was found to decrease with increasing kanamycin concentration (Figures 1c-d, Figure 2b). Moreover, the velocity distribution was found to continuously shift from a Gaussian, to nearly an exponential tail – a Laplace distribution (Figure 2c). Figure 2d shows the normalized forth moment (kurtosis) of the distribution curves, changing from 3 (Gaussian) for antibiotics-free samples to 6 (exponential tail) and even larger at high kanamycin concentrations.

To further investigate the statistics of the collective swarm dynamics we analyzed correlation functions. Spatial correlations decay exponentially and the characteristic length scale does not depend on antibiotic concentration, see Figure S1. The typical tool for quantifying temporal correlations is the velocity correlation function, $C(t) = \langle \bar{v}(s,\bar{x}) \cdot \bar{v}(s+t,\bar{x}) \rangle$, where $\bar{v}(t,\bar{x})$ denotes the velocity field at time t and position $\bar{x} \in \mathbb{R}^2$. Brackets denote averaging over all times (all frames in the recorded movies) and positions (a 64×64 grid on each image). However, the velocity correlation function is strongly biased towards elements with a high speed. Inparticular, it cannot detect if particles (or positions) with low speeds behave differently than those with high speeds. This is because the contribution of low-speed particles is small. To this end, we consider the directional correlation function defined as

$$\hat{C}(t) = \langle \hat{v}(s,\bar{x}) \cdot \hat{v}(s+t,\bar{x}) \rangle \,, \tag{1}$$

where $\hat{v}(t,\bar{x})$ is the normalized velocity or direction vector, $\hat{v}(t,\bar{x}) = \bar{v}(t,\bar{x})/|\bar{v}(t,\bar{x})|$. For similar or alternative definitions of directional correlations see [29, 30]. Under Boltzmann statistics (e.g., a particle under Langevin dynamics) the decay of $\hat{C}(t)$ is not exponential. However, it has an exponential tail and can be approximated by a double exponential decay of the form $\hat{C}(t) = I_{\rm slow} e^{-t/\tau_{\rm slow}} + I_{\rm fast} e^{-t/\tau_{\rm fast}}$ such that $I_{\rm slow} + I_{\rm fast} = 1$. Fitting $\hat{C}(t)$ to the experimental data we identified two distinctive time scales $\tau_{\rm slow} = 0.2$ sec and $\tau_{\rm fast} = 0.015$ sec that only weakly depend on antibiotics concentration (Figures 3a and S2). In the absence of antibiotics, $I_{\rm slow} \sim 10 I_{\rm fast}$, as expected under Boltzmann statistics. However, the more kanamycin is added, the contribution of the fast relaxation becomes larger (Figure 3b).

We hypothesize that low concentrations of kanamycin disable the motility of a fraction f of the cells, ranging from $f = 0$ to 1 with added antibiotics. At large concentrations (0.1 μg/l) all cells should arrest, as all have had critical proteins sufficiently diluted by growth and turnover. However, at sub-lethal concentrations cell systems fail stochastically as each cell has an a-priori sensitivity threshold taken from some distribution. Kanamycin should inhibit de novo synthesis of proteins (flagellin) and motile cells will thus be diluted.

Motile-immotile mixtures. To test our hypothesis regarding the effect of kanamycin, genetically engineered immotile *B. subtilis* mutants were mixed with WT colonies at a range of ratios. immotile cells were labeled with a red fluorescent protein (RFP) marker in order to estimate the exact ratio (details in SM).

Figure 4 shows experimental results with motile-immotile mixtures, which are in agreement with the antibiotics experiments. A precise comparison between the two experiments is difficult because the fraction of immotile cells at a given antibiotics concentration is unknown. The large similarity between the experiments leads us to conclude that the antibiotics stress disrupts the coherence of the bacterial motion by creating a population of motility-defective bacteria among the healthy ones.

Modeling and simulations. In order to identify the key physical processes underlying the dynamics, we suggest a simplified model of a binary mixture of inelastic spheres (see also [30]). Consider unit mass particles with radius r moving in a two-dimensional square domain $[0, L]^2$ with periodic boundary conditions. Denote the positions and velocities at time t by $x_1, \ldots, x_N$ and $v_1, \ldots, v_N$. Each particle undergoes Langevin dynamics, i.e., its velocity is an Ornstein-Uhlenbeck process,

$$\dot{x}_i = v_i \ , \quad \dot{v}_i = -\frac{1}{\tau_i} v_i + \sqrt{\frac{2T_i}{\tau_i}} \dot{W}_t^i, \tag{2}$$

where $\dot{W}_t^i$, $i = 1 \ldots N$ are independent white noise, τ_i are the deceleration times (τ_i^{-1} are the viscosity coefficients), which may be different for different particles.

The variance in v_i is T_i. We assume that particles are divided into two sub-populations: particles $1 \dots N_1$ are motile while particles $N_1 + 1 \dots N$ are immotile. The fraction of motile particles is $f = N_1/N$. The motility of particles affects both the local viscosity, τ_i^{-1} , and the amount of pushing, i.e., the diffusivity, T_i. Accordingly, each population is characterized by different parameters τ and T,

$$\tau_i = \begin{cases} \tau_{\rm m} & i \le N_1 \\ \tau_{\rm im} & i > N_1 \end{cases}, T_i = \begin{cases} T_{\rm m} & i \le N_1 \\ T_{\rm im} & i > N_1 \end{cases}, \qquad (3)$$

where $\tau_{\rm m} > \tau_{\rm im}$ (motility reduces viscosity [9]) and $T_{\rm m} > T_{\rm im}$ (motile particles are more driven). The two time scales correspond to the experimentally observed scales $\tau_{\rm slow}$ and $\tau_{\rm fast}$. Two particles that get to a distance $2r$ between each other collide inelastically with a restitution coefficient that depends on the type of particles, $\beta_{\rm im,im} < \beta_{\rm m,im} < \beta_{\rm m,m}$, see SM. One possible explanation for the different restitution coefficient is a different composition of the fluid and proteins surrounding the bacteria.

The model presents a highly simplified version of the motile-immotile experiments and neglects a wide range of physical properties of bacteria, such as the elongated shape of cells and the flagellar degrees of freedom. Nonetheless, comparison between the experimental and simulated results, depicted in Figures 4 and S3, show an excellent quantitative agreement. Parameters were fitted to capture the experimental data (see SM).

Permanent vs. temporary transitions. Experiments show that in antibiotics treated plates, cells aggregate together, forming relatively static clusters or islands, while other bacteria move between them (see red lines in Figures 1a,c). This observation can be quantified in simulations, in which the precise particle trajectories are known. To this end, we define a cluster of particles as follows. We refer to two particles as neighbors at time t if the distance between them is smaller than a threshold $r_{\rm c}$ for longer than a given time segment $T_{\rm c}$, i.e., if $\max_{s\in[t-T_{\rm c},t]} |x_i(s) - x_j(s)| \le r_{\rm c}$. In simulations, we take $r_{\rm c} = 3r$ and $T_{\rm c} = 0.5$ sec. Consider the adjacency graph at time t, i.e., a graph with particles as vertices and edges between neighbors (see SM). Connected components of the adjacency graph at a given time t with more than two particles are considered clusters. In a system of $50 - 50$ motile and immotile particles ($N = 200$), 6.3% of motile particles belong to a cluster compared to 53.9% of immotile particles (on average). This supports the observation that the system partially self-separates into zones of motile and immotile bacteria. Therefore, the appearance of islands, corresponding to immotile, antibiotics affected bacteria, is explained in terms of the physical properties of granular materials, in our case, a binary mixture of hard spheres colliding inelastically. In other words, it is a physical phenomenon, rather than a biological one.

A key question is whether the classification of each cell is permanent or varying. In the first case, each cell is either permanently affected by antibiotics (within the experimental time) or not. In the second, cells may switch their state at random times. The latter scenario is particularly appealing as it offers an alternative explanation for the non-exponential decay of correlations as a heavy-tail distribution of waiting times for switching between motile and immotile states. To test this hypothesis, we randomly permute the type of particles (motile or immotile) in the model. Figure 4d shows the fraction of motile and immotile particles that are members of clusters (with more than one particle) as a function of permutation rate, $k_{\rm permute}$. We find that permutations have a drastic effect on clustering. Intuitively, a clustered immotile particle that suddenly becomes motile can break up a cluster. On the other hand, motile particles becoming immotile take time to cluster and aggregate. The non-monotonic curve for the immotile particles indicates that below a threshold rate, clusters of immotile particles start appearing. This supports our assumption that the sub-population of immotile bacteria is fixed.

The rate in which bacteria switch between motility states dictates the fraction of free motile bacteria. At high switching rates, the mixing of motile and immotile cells disturbs coherent motion and prohibits expansion. At low rates, immotile cells cluster, allowing free-swimming bacteria to expand.

The role of inelastic collisions. Transition from Gaussian distribution can also be due to inelastic inter-particle collisions [30, 31]. However, inelastic collisions on their own have an opposite effect than observed in our experiments as antibiotics reduces the average speed of cells, therefore reducing collision rates and the significance of collisions.

Summary. The physical differences between motile and immotile cells cause the system to segregate into regions characterized by a high fraction of either motile or immotile cells. As swarming is a collective behavior that requires a high density of motile bacteria, the spatial segregation enables motile bacteria to swarm efficiently even though their overall density is significantly reduced. This is supported by our observation that, indeed, the growth rate of the entire colony is not affected by antibiotics. In other words, changing the physical properties of the cells and the local fluid surrounding it can be thought as a strategy bacteria employ to fight sub-lethal antibiotic concentrations.

At higher kanamycin concentrations (> 0.08 μg/ml), the response to antibiotics becomes more complicated and additional biological effects need to be taken into account. For example, comparing Figures 2d with 4b, the 4th moment with antibiotics can be larger than 6, indicating that the tail of the velocity distribution function decreases slower than exponentially. This behavior cannot be seen with experiments or simulations of motile-immotile mixtures.

We thank Daniel B. Kearns for providing us with the

WT and immotile cells and for useful discussions. We also thank Avigdor Eldar and Shaul Pollak for creating the RFP mutants. We thank Eli Ben-Naim, Rasika M. Harshey, David Kessler and Dalit Roth for useful discussions and suggestions. EB-J thanks partial support from the Tauber Family Funds and the Maguy-Glass Chair in Physics of Complex Systems at Tel Aviv University. GA thanks partial support from an EU/FP7 Marie-Curie IRG grant. AB thanks partial support from an EU/FP7 REA grant 321777, The Israel Science Foundation (grant No. 337/12) and the Roy J. Zuckerberg Career Development Chair for Water Research.

[1] R.M. Harshey, Annu. Rev. Microbiol., **57**, 249 (2003); A. Be'er and R.M. Harshey, Biophys. J. **101**, 1017 (2011); J.D. Partridge and R.M. Harshey, J. Bacteriol. **195**, 909 (2013);
[2] H.P. Zhang *et al.*, Proc. Natl. Acad. Sci. USA **107**, 13626 (2010).
[3] H.P. Zhang *et al.*, Europhys. Lett. **87**, 48011 (2009).
[4] X. Chen *et al.*, Phys. Rev. Lett. **108**, 148101 (2012).
[5] D.B. Kearns and R. Losick, Mol. Microbiol. **49**, 581 (2004); D.B. Kearns, Nat. Rev. Microbiol. **8**, 634 (2010).
[6] Y. Wu, B.G. Hosu and H.C. Berg, Proc. Natl. Acad. Sci. USA **108**, 4147 (2011).
[7] M.F. Copeland and D.B. Weibel, Soft Matter 5, 1174 (2009).
[8] S. Zhou *et al.*, Proc. Natl. Acad. Sci. USA **111**, 1265 (2014).
[9] A. Sokolov and I.S. Aranson, Phys. Rev. Lett. **103**, 148101 (2009).
[10] T. Ishikawa *et al.*, Phys. Rev. Lett. **107**, 028102 (2011).
[11] J. Dunkel *et al.*, Phys. Rev. Lett. **110**, 228102 (2013).
[12] H.H. Wensink *et al.*, Proc. Natl. Acad. Sci. USA **109**, 14308 (2012).
[13] A. Rabani, G. Ariel and A. Be'er, PLoS One **8**, e83760 (2013).
[14] A. Sokolov and I.S. Aranson, Phys. Rev. Lett. **109**, 248109 (2012).
[15] A. Be'er *et al.*, J. Bacteriol. **191**, 5758 (2009).
[16] N.G. Kamatkar and J.D. Shrout, PLoS One **6**, e20888 (2011).
[17] M.T. Butler, Q. Wang and R.M. Harshey, Proc. Natl. Acad. Sci. U. S. A. **107**, 3776 (2010).
[18] D. Roth *et al.*, Environ. Microbiol. **15**, 2532 (2013).
[19] S. Lai, J. Tremblay and E. Déziel, Environ. Microbiol. **11**, 126 (2009).
[20] E. Lushi, H. Wioland and R.E. Goldstein, Proc. Natl. Acad. Sci. USA **111**, 9737 (2014); C. Dombrowski *et al.*, Phys. Rev. Lett. **93**, 098103 (2004); A. Sokolov *et al.*, Phys. Rev. Lett. **98**, 1 (2007); L.H. Cisneros *et al.*, Exp. Fluids **43**, 737 (2007); V. Gyrya *et al.*, Bull. Math. Biol. **72**, 148 (2010);
[21] G. Ariel *et al.*, New J. Phys. **15**, 125019 (2013).
[22] M.F. Copeland *et al.*, Appl. Environ. Microbiol. **76**, 1241 (2010).
[23] C.J. Ingham and E. Ben Jacob, BMC Microbiol. **8**, 1 (2008).
[24] H.H. Tuson *et al.*, J. Bacteriol. **195**, 368 (2013).
[25] A. Be'er *et al.*, J. Bacteriol. **195**, 2709 (2013).
[26] F. Peruani, A. Deutsch and M. Bär, Phys. Rev. E **74**, 030904 (2006).
[27] D. Grossman, I.S. Aranson, and E. Ben Jacob, New J. Phys. **10**, 023036 (2008).
[28] F. Peruani and L. Morelli, Phys. Rev. Lett. **99**, 010602 (2007).
[29] S. Burova, S.M.A. *et al.*, Proc. Natl. Acad. Sci. U. S. A. **110**, 19689 (2013).
[30] E. Ben-Naim and P.L. Krapivsky, *Lecture Notes in Physics* **624**, 65 (2003).
[31] K. Kohlstedt *et al.*, Phys. Rev. Lett. **95**, 068001 (2005).

Figures

FIG. 1: *B. subtilis* swarming colonies. Left: Top-view phase contrast microscopic image of a swarm taken close to the colony's edge. Red lines separate regions of very slowly moving cells (static clusters) from fast moving cells. (a) No added antibiotics. Regions encircled by red are stationary. (c) With added 0.08 μg/ml kanamycin. Regions encircled by red are moving. Right: The instantaneous velocity field at the same time. Colors indicate clockwise (red) or counter-clockwise (blue) motion. (b) No added antibiotics and (d) with added 0.08 μg/ml kanamycin. The scale bar is 10 μm.

FIG. 2: The effects of kanamycin. (a) Number of CFU (live bacteria) at the colony edge using three different measurment methods (red, blue and green) and the average expansion rate of the colony (black), indicating that the colony's expansion is not affected. (b) The average speed of the swarm gradually decreases with added kanamycin. (c) The centered distribution of the x and y components of the velocity. The 0 kanamycin curve is Gaussian. (d) The scaled forth moment (kurtosis) of the velocity distribution functions changes from 3 (Gaussian) for antibiotics-free samples to 6 (exponential tail) and even larger at high concentrations.

FIG. 3: A double exponential decay in the directional correlation function $\hat{C}(t)$. (a) A close to exponential decay for the 0 kanamycin case (black curve). A double exponential decay for the 0.08 μg/ml kanamycin case (gray curve). The two time scales weakly depend on antibiotics concentration (Figure S2). (b) The contribution (amplitudes) of each exponent as a function of kanamycin. The relative contribution of each time scale switches from mostly slow to mostly fast at around 0.075 μg/ml kanamycin.

FIG. 4: Experimental (dots) and simulation (lines) results for mixtures of motile and immotile cells. (a) The mean speed, (b) the kurtosis of the velocity distribution and (c) amplitudes of the double exponential decay in the directional correlation function $\hat{C}(t)$. Compare with the antibiotics treated experiments Figs. 2a,c and Fig. 3b. (d) The fraction of motile and immotile particles taking part of clusters as a function of permutation rate. Points on the y-axis indicate the no-permutation case. At high rates, and immotile particles behave similarly. However, at sufficiently low rates the system self-segregates into immotile clusters and motile particles moving between them.

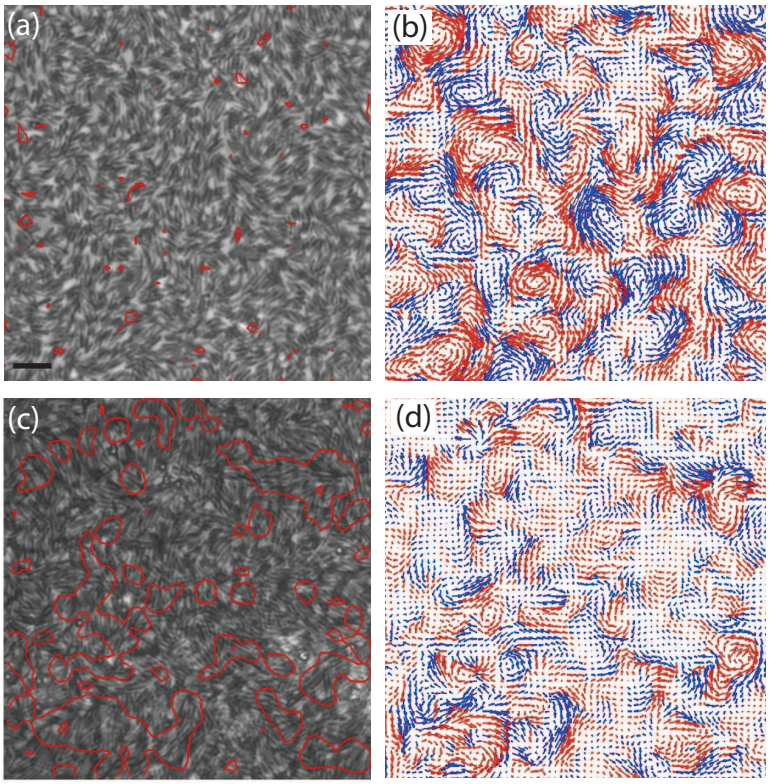

Figure 1 16Dec2014

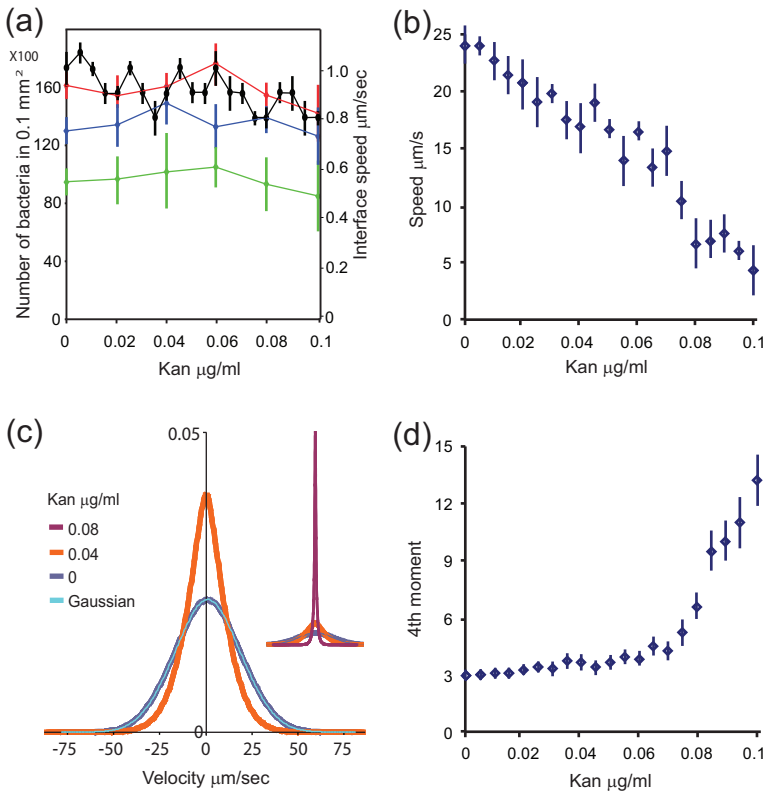

Figure 2 16Dec2014

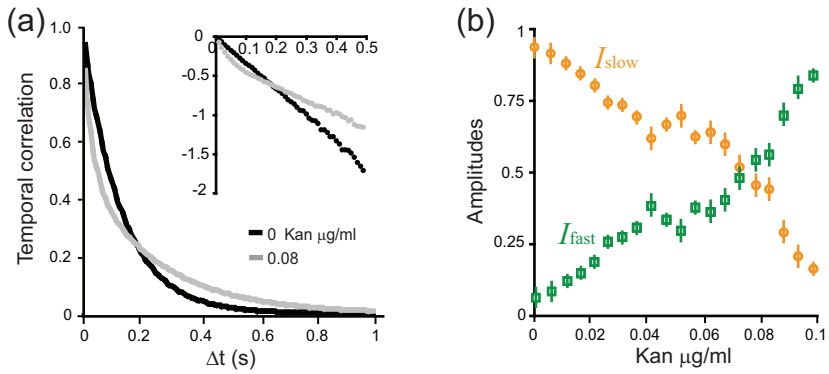

Figure 3 16Dec2014

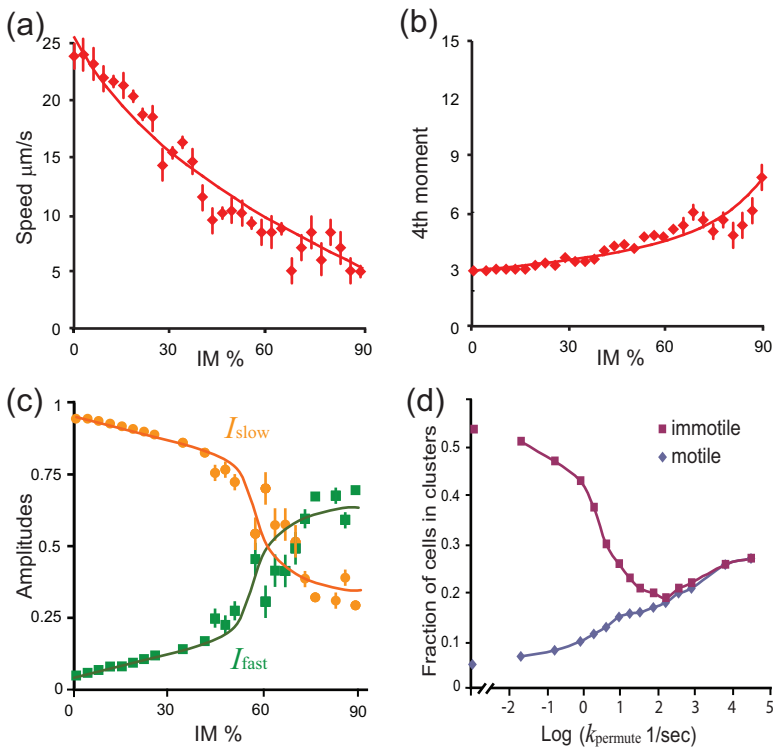

Figure 4 16Dec2014